Investigation on the Failure Mechanisms in Sandstones under Uniaxial Compression by Digital Image Correlation

Ganyun Huang*, Hao Zhang, Haipeng Song, Yilan Kang

Department of Mechanics, Tianjin University, Tianjin 300072, China
* Corresponding author: g.y.huang@hotmail.com

Abstract Sandstone samples have been compressed uniaxially till failure. The displacement field during the deformation process has been obtained by digital image correlation (DIC) technique. It has been observed that the rock samples ruptured through splitting parallel to the compression direction, as conventional experiments indicated. But upon analyzing the apparent strain field, no sliding cracks or shear cracks have been found that are suggested to drive the splitting failure. Instead, deformation band like structure has been detected. The splitting failure has been observed to be the direct result of the localization of the some scattered small cracks. The micromechanism underlying may be the buckling of force chains that induces delamination between them.

Keywords uniaxial compression, failure mechanism, sandstone, digital image correlation

1. Introduction

The failure of rocks under compression may hold important implications in many aspects such as geophysics, civil engineering and mining sciences. In fact, uniaxial compressive strength has even been a key parameter in estimating the performance of cutters in rock drilling. Despite the wide variety of rock types, a large body of experiments have demonstrated the rock fails under uniaxial compression via axial splitting or shear faulting [1-4]. Such macroscopic failure mode can be well explained by the nucleation and propagation of the wing cracks that is assumed to depend on the existence of sliding cracks. Experiments on samples with pre-existing cracks, or more exactly cuts inclined to the compression direction have also proved the wing crack formation and propagation that leads to axial splitting [5-7]. Model of wing crack formation and propagation has been widely applied to the damage and micromechanics of rock like brittle materials [8-11]. However, the model depends critically on the existence of sliding or shear cracks. No experiments have been reported on the nucleation of the shear cracks. Thus what the physical micromechanisms drive the axial splitting under uniaxial compression remains an open question.

In rock like brittle materials, it has been conventionally believed that microcracks with a random distribution of various orientations exist, which may make the nucleation of sliding cracks dispensable. If it is true, then analyzing the full-field deformation behavior of as-received rock samples under uniaxial compression may help to reveal splitting induced by the sliding crack or the physical micromechanisms for axial splitting. Combination of the uniaxial compression test and DIC technique may suit the purpose very well. Indeed, through DIC technique, full field displacement on the sample surface can be obtained efficiently without contact and hence damage. Applicability of the technique to the rock deformation has already been demonstrated in our previous work [12]. Thus, we will use DIC technique to study the deformation behavior of rocks under uniaxial compression so as to cast some new light on the failure mechanisms at microscopic level.

2. Experiments

Samples of dimension 25×25×50 mm were cut from a large sandstone block from Yunnan, China. All the sample surfaces were randomly painted with artificial speckles. Then the sandstone samples were uniaxially compressed along the longest sides on the electric universal machine

(CSS-44100). Compressive load was controlled by displacement mode at a speed of 0.06mm/min. During the whole loading stage, a CCD camera (1004×1003 pixels, 8bits) under the illumination of two light sources was installed perpendicularly to the samples so as to capture the images that were simultaneously stored on a computer disc for subsequent processing. The length-pixel ratio of the images is 61.7μm/pixel and recording frequency was 1frame/s. It is worth mentioning that only the images in the area as indicated by the white rectangle in Fig.1(a) will be used to obtain the displacement fields. The experimental setup is illustrated in Fig.1(b).

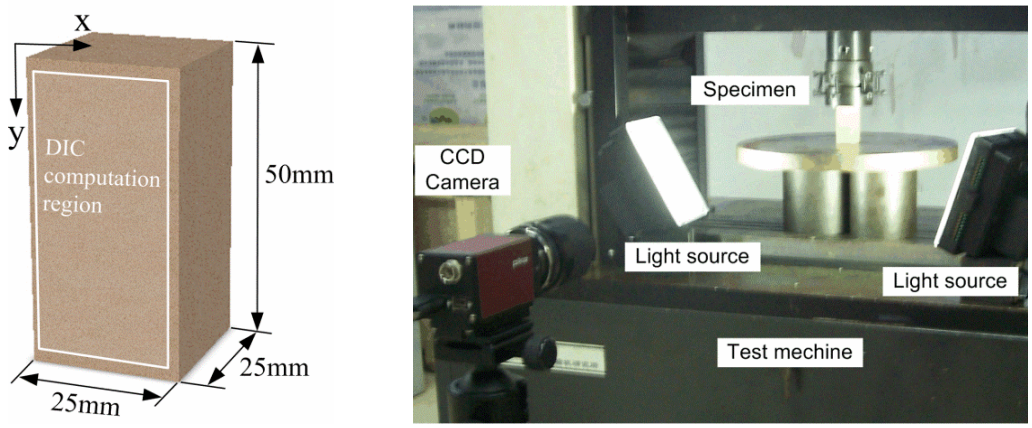

(a) (b)

Fig.1 (a) sandstone sample and (b) experimental setup

In the present work, the image was processed by our in-house DIC software. A relatively small calculation subset size (21×21 pixels) and step length (10 pixels) were chosen to increase the spatial resolution of the measurement. The displacement measurement accuracy in our test was at least 1μm based on our calibration.

3. Results and discussions

The load-displacement (at the contact interface) recorded by the electric universal machine is present in Fig. 2. It can be seen that except at the initial stage, the load is almost proportional to the displacement even till failure (with macroscopic crack). The sample fails at a load level of about 68kN via axial splitting.

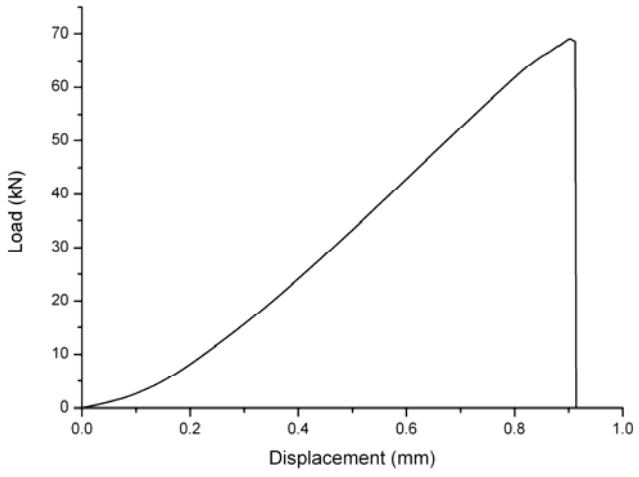

Fig.2 Load-displacement curve during the uniaxial compression of a sandstone sample

Using the DIC technique as handled in [12], we have obtained the displacement fields in the region indicated by the white rectangle in Fig. 1(a). Distributions of the displacements at load levels of 40, 55, 62, 62.7 and 64.5 kN have been presented respectively in Fig.3.

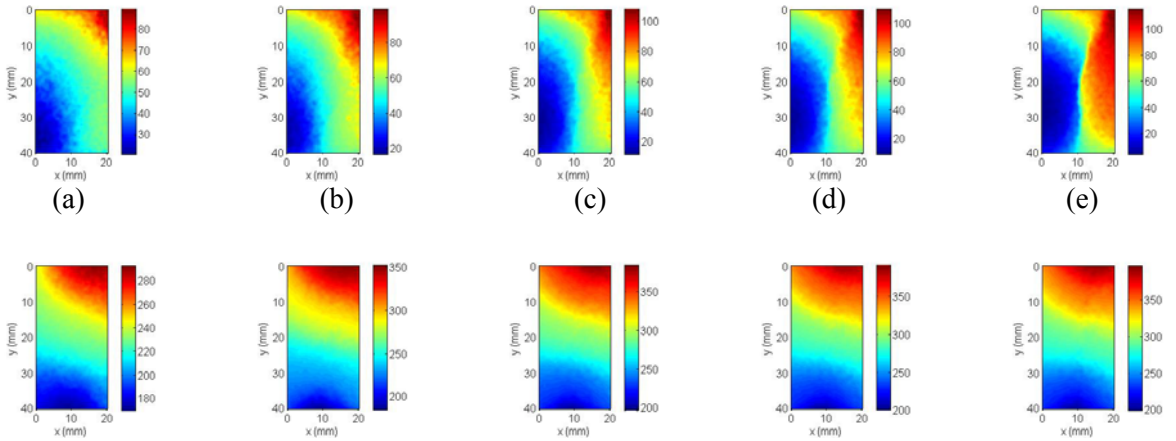

Fig.3 The horizontal (a-e) and vertical (f-j) displacements on the sample surface at load levels of 40, 55, 62, 62.7 and 64.5 kN respectively (unit in the legend is micron)

The displacement distributions clearly indicate uneven deformation has occurred especially when the applied load is close to the rupture load where the color pattern for the horizontal displacement is highly discontinuous at the middle of the sample. Partially the inhomogeneous deformation may be induced by the micro-structure in the sandstone. Observations by optical microscopy have indeed shown the sandstone is composed of grains of microns but the grain size is rather homogeneous (results not shown). It may also be the result inherent to the sandstone. To better analyze the deformation behavior, the apparent strain on the surface has been calculated since when there are cracks, displacement jumps may appear due to the crack faces sliding and opening and induce large apparent strain.

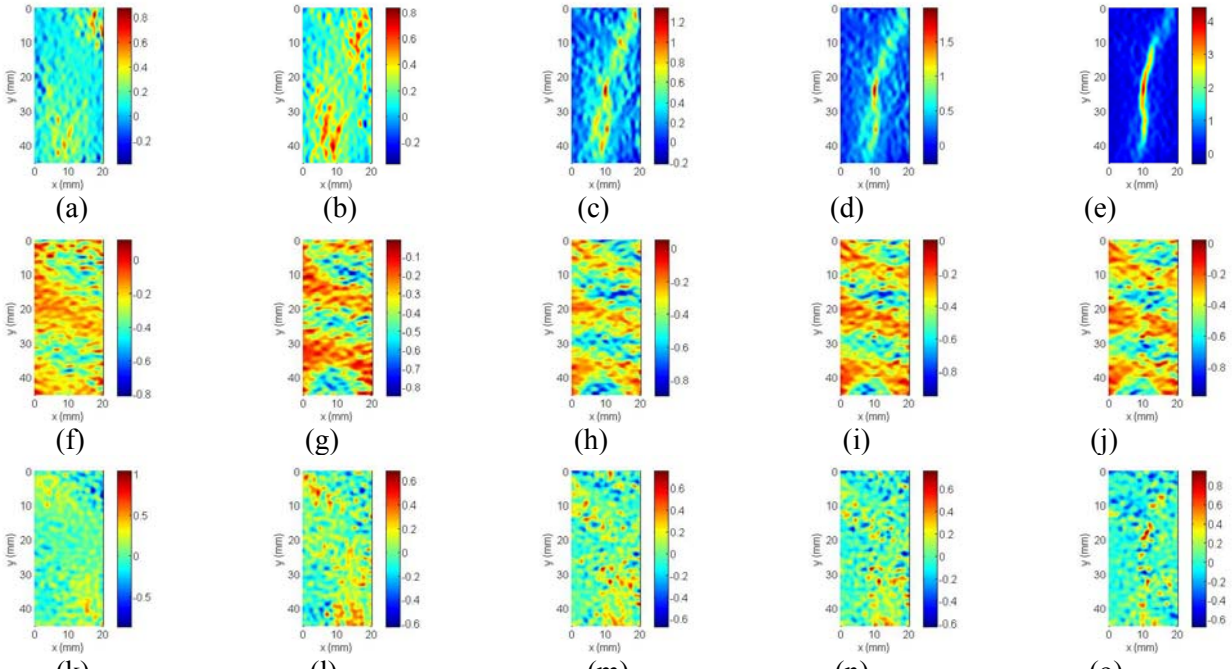

Fig. 4 apparent ε_{xx} (a-e), ε_{yy} (f-j) and γ_{xy} (k-o) on the sample surface at load levels of 40, 55, 62, 62.7 and 64.5 kN respectively (The values are in percentage)

The apparent strain distributions corresponding to load levels of 40, 55, 62, 62.7 and 64.5 kN respectively have been demonstrated respectively in Fig. 4. The apparent ε_{xx} at a given load level is inhomogeneous. The regions with apparent ε_{xx} value much larger than the average are highly localized and somewhat scattered at relatively lower load levels. For example, see Fig.4 (a) and (b). Such regions may be considered as locally split given the much larger than average values of the apparent ε_{xx}. With the increase in compressive load, the regions with apparent ε_{xx} much larger than the average become to join up and are distributed almost along a line inclined to the loading direction as shown in Fig. 4(d). Close to the rupture load, the regions with relatively large value of apparent ε_{xx} are distributed along a line and from the color pattern in Fig. 4(e) look like a macroscopic crack. The final rupture actually did propagate along that line. The apparent ε_{yy} behaves completely different. The area of interest as indicated in Fig. 1(a) is alternated with regions of small apparent ε_{yy} (nearly not deformed) and those of larger apparent ε_{yy}. Deformation band structure forms. The number of bands increases with compressive load. The bands tend to be broken at the middle along a vertical line, possibly due to the damage leading to splitting. Distribution of the apparent engineering shear strain γ_{xy} is also localized but much more scattered than that of apparent ε_{xx}. In most cases, the largest magnitude of the apparent shear strain is smaller than those of apparent ε_{xx} and apparent ε_{yy}. In fact, at relatively large compressive load, the apparent ε_{xx} has the largest magnitude among all the apparent strain components on the surface. It may be the result from the axial splitting and so the apparent strain ε_{xx} can be conveniently used for identification of cracking and damage in our experiments.

The deformation band structure in the apparent ε_{yy} appears rather unexpected although compaction bands or shear bands have been observed in rocks with high porosity and usually under confinement [13, 14]. Because the porosity in our samples is very low (about 5%), the formation of deformation band can hardly be attributed to the sandstone compaction. Moreover, the banded structure evolves with compressive load even at levels larger than 30 kN, see Fig.4 (f-j) and no hardening behavior has been found in Fig.2 at those load levels. We have also excluded the possibility of artificial factors. Other algorithm has been adopted to calculate the apparent ε_{yy} but with similar results despite the slight difference in magnitude (results now shown). Besides, the precision for displacement measurement is adequate given the high levels of loading applied in those results. The formation of band structure in ε_{yy} may affect the failure behavior of the present sandstones under uniaxial compression. Conventionally, axial splitting has been explained by formation and propagation of wing cracks that depends on the existence of a sliding crack or shear crack. However, no evidence for that has been detected. Before the final rupture via axial splitting, if there were sliding microcracks, the apparent shear strain would be very large and dominant over other apparent strain components at the crack faces. However, as mentioned above, the apparent ε_{xx} has the largest magnitude in those situations. The line along which the much-larger-than-average apparent strain ε_{xx} is distributed seems to be consistent with the shear plane predicted by Mohr-Coulomb strength criterion. But it cannot result from shear but rather from the coalescence of the relatively scattered and local splitting.

With in mind that Bazant et al has suggested that under uniaxial compression splitting crack band may form which would subsequently result in the formation of column bundles [15], we have enlarged the displacement by fifty times so as to visualize the deformed profile of the area of interest. The results are demonstrated in Fig.5. Dash blue lines are plotted only guided eyes. If the material points distributed along a line with same x can be considered a column, then one may find that the area of interest deforms by compressing the columns and some of them *buckled* locally. By scrutinizing the results in Fig. 5, one may also notice that the buckled regions are correlated with

the banded structure in the apparent ε_{yy}. Moreover, the axial splitting may be driven by the buckling induced delamination between the columns. Thus it is likely deformation of the present sandstone under compression can be described by force chain model as applied in mechanics of granular materials [16]. However, more detailed experiments are required to confirm it and whether such a failure mechanism is applicable to other brittle rocks under uniaxial compression remains for future study.

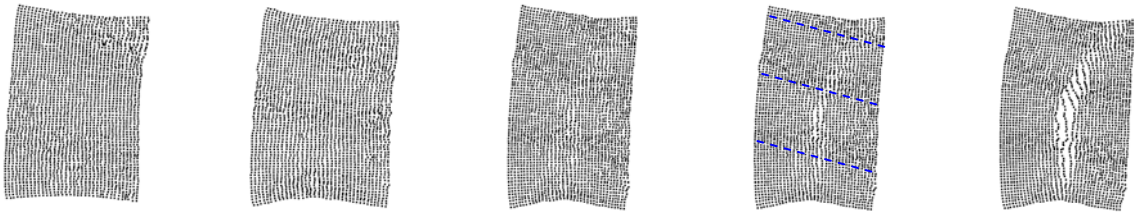

(a) (b) (c) (d) (e)

Fig. 5 Visualization of the deformed profile by zooming out displacement by 50 times at load level of 40, 55, 62, 62.7 and 64.5 kN (The difference in width and height is caused by different display ratio)

4 Concluding remarks

Samples of sandstone under uniaxial compression were studied experimentally by combing the conventional compressive test with DIC technique. Deformation field and its evolution with loading have been obtained with the aid of DIC technique. It has been found the sandstone deformed in an inhomogeneous manner and failed via axial splitting. However the failure mode cannot be attributed to the wing crack formation and nucleation. Instead, the macroscopic crack formed via coalescence of some local axial splitting microcracks and the micromechanism may be the buckling of force chains that induces delamination. Although more detailed experiments are required to verify it, the present results may cast new light on understanding the failure mechanism in brittle materials under compression.

Acknowledgements

This work was supported by the National Natural Science Foundation of China under Grant Nos.11072170 and 11127202.

References

[1] J. Gramberg, Axial cleavage fracturing, a significant process in mining and geology. Eng. Geol., 1(1965) 31-72.
[2] S. Peng, A. M. Johnson, Crack growth and faulting in cylindrical specimens of Chelmsford granite. Int J Rock Mech Min Sci., 9(1972) 37-86.
[3] M. S. Paterson, Experimental deformation and faulting in Wombeyan marble. Bull. Geol. Soc. Am. 69(1958) 465-76.
[4] B. T. Brady, Theory of earthquakes. I. A scale independent theory of rock failure. Pure Appl Geophs. Res., 112(1974) 701-25.
[5] E. Z.Lajtai, Brittle failure in compression. Int. J. Fract., 10(1971) 525 – 536.
[6] H. Horii, S. Nemat-Nasser, Brittle failure in compression: splitting, faulting and brittle-ductile transition. Phil. Trans. R. Soc. Lond. A., 319(1986) 337-374.
[7] A. Bobet, H. H. Einstein, Fracture coalescence in rocktype materials under uniaxial and biaxial compression. Int. J. Rock Mech. Min. Sci., 35(1998) 863-888.

[8] Y. Okui, H. Horii, Stress and time-dependent failure of brittle rocks under compression: A theoretical prediction. J. Geophys. Res., 102(1997) 14869-14881.
[9] H. B. Li, J. Zhao, T. J. Li, Micromechanical modeling of the mechanical properties of a granite under dynamic uniaxial compressive loads. Int. J. Rock Mech. Min. Sci., 37(2000) 923-935.
[10] B. Paliwal, K. T. Ramesh, An interacting micro-crack damage model for failure of brittle materials under compression. J. Mech. Phys. Solids., 56(2008) 896 – 923.
[11] H. S Bhat, C. G.Sammis, A. J. Rosakis, The micromechanics of Westerley granite at large compressive loads. Pure Appl. Geophys. ,168(2011) 2181–2198
[12] H. Zhang, G. Huang, H. Song, Y. Kang, Experimental investigation of deformation and failure mechanisms in rock under indentation by digital image correlation. Eng Fract Mech., 96(2012) 667-675.
[13] P. Baud, S. Vinciguerra, C. David, A. Cavallo, E. Walker, T. Reuschle, Compaction and failure in high porosity carbonates: Mechanical data and microstructural observations. Pure Appl. Geophys., 166(2009) 869-898
[14] V. Vajdova, W. Zhu, T. M. N. Chen, T. Wong, Micromechanics of brittle faulting and cataclastic flow in Tavel limestone. J.Struct. Geol., 32(2010) 1158-1169.
[15] Z. P. Bazant, Y. Xiang, Size effect in compression fracture: splitting crack band propagation. J. Eng. Mech., 123(1997) 162-172.
[16] S. Ostojic, E. Somfai, B. Nienhuis, Scale invariance and universality of force networks in static granular matter. Nature, 439(2006) 828-830.